



HAL
open science

Modulated Linear Tellurium Chains in Ba₃ScTe₅: Synthesis, Crystal Structure, Optical and Resistivity Studies, and Electronic Structure

Mohd Ishtiyak, Gopabandhu Panigrahi, Subhendu Jana, Jai Prakash, Adel Mesbah, Christos Malliakas, Sébastien Lebègue, James Ibers

► **To cite this version:**

Mohd Ishtiyak, Gopabandhu Panigrahi, Subhendu Jana, Jai Prakash, Adel Mesbah, et al.. Modulated Linear Tellurium Chains in Ba₃ScTe₅: Synthesis, Crystal Structure, Optical and Resistivity Studies, and Electronic Structure. *Inorganic Chemistry*, 2020, 59 (4), pp.2434-2442. 10.1021/acs.inorgchem.9b03319 . hal-03005937

HAL Id: hal-03005937

<https://hal.science/hal-03005937>

Submitted on 23 Nov 2020

HAL is a multi-disciplinary open access archive for the deposit and dissemination of scientific research documents, whether they are published or not. The documents may come from teaching and research institutions in France or abroad, or from public or private research centers.

L'archive ouverte pluridisciplinaire **HAL**, est destinée au dépôt et à la diffusion de documents scientifiques de niveau recherche, publiés ou non, émanant des établissements d'enseignement et de recherche français ou étrangers, des laboratoires publics ou privés.

Modulated Linear Te-chains in Ba₃ScTe₅: Synthesis, Crystal Structure, Optical, Resistivity Studies, and Electronic Structure

Mohd Ishtiyak,[†] Gopabandhu Panigrahi,[†] Subhendu Jana,[†] Jai Prakash,^{†,‡} Adel Mesbah,^{‡,§} Christos D. Malliakas,[‡] Sébastien Lebègue,[‡] and James A. Ibers^{‡,*}

[†]Department of Chemistry, Indian Institute of Technology Hyderabad, Kandi, Sangareddy, Telangana 502285, India

[‡]Department of Chemistry, Northwestern University, 2145 Sheridan Road, Evanston, IL 60208-3113, United States

[§] ICSM, Univ Montpellier, CEA, CNRS, ENSCM, Site de Marcoule, Bagnols-sur-Cèze, France

[‡]Laboratoire de Physique et Chimie Théoriques (LPCT, UMR CNRS 7019), Institut Jean Barriol, Université de Lorraine, BP 239, Boulevard des Aiguillettes, Vandoeuvre-lès-Nancy 54506, France

ABSTRACT: A new ternary telluride, Ba₃ScTe₅, with a pseudo one-dimensional structure, was synthesized at 1173 K by standard solid-state methods. A single-crystal X-ray diffraction study at 100(2) K shows the structure to be modulated. The structure of the subcell of Ba₃ScTe₅ crystallizes with two formula units in the hexagonal space group $D_{3h}^3-P6_3/mcm$ with unit cell dimensions of $a = b = 10.1190(5)$ Å and $c = 6.8336(3)$ Å. The asymmetric unit of the subcell structure consists of four crystallographically independent sites: Ba1 (site symmetry: $m2m$), Sc1 ($-3.m$), Te1 ($m2m$), and Te2 (3.2). Its structure is made up of chains of $^{1,\infty}[\text{ScTe}_3^{3-}]$ that are separated by Ba²⁺ cations. The Sc atoms are bonded to six Te1 atoms that form a slightly distorted octahedral geometry. The structure of subcell also contains linear infinite chains of Te2 with intermediate Te⋯Te interactions. The superstructure of Ba₃ScTe₅ is incommensurate and was solved in the hexagonal superspace group $P-6(00\gamma)0$ with $a = 10.1188(3)$ Å and $c = 6.8332(3)$ Å and a modulation vector of $q = 0.3718(2)c^*$. The arrangement and coordination geometries of atoms in the superstructure are very similar to those in the substructure. However, the main difference is that the infinite chains of Te in the superstructure are distorted owing to the formation of long- and short-bonded pairs of Te atoms. The presence of these chains with intermediate Te⋯Te interactions makes the assignment of formal oxidation states arbitrary. The optical absorption study of a polycrystalline sample of Ba₃ScTe₅ that was synthesized by the stoichiometric reaction of elements at 1173 K reveals a direct bandgap of 1.1(2) eV. The temperature-dependent resistivity study of polycrystalline Ba₃ScTe₅ shows semiconducting behavior corroborating the optical studies while DFT calculations report a pseudo bandgap of 1.3 eV.

INTRODUCTION

The study of structure-property relationships of transition metal chalcogenides is an active area in solid-state chemistry owing to a variety of applications to thermoelectric properties, magnetism, superconductivity, magnetoresistance, and charge density waves (CDW).¹⁻⁵ The ternary and quaternary compounds such as Ba_2MnQ_3 ,⁶ $(\text{BaF})_2\text{Fe}_{2-x}\text{Q}_3$,⁷ and AFeS_2 ($A = \text{K}$ and Rb)⁸ are examples that show interesting magnetic behavior. Furthermore, layered structures such as $\text{K}_2\text{Cu}_5\text{Te}_5$,³ MQ_2 ($M = \text{V}, \text{Nb},$ and Ta ; $Q = \text{S}, \text{Se},$ and Te),⁹ PtTe_2 ¹⁰ are metallic, and compounds like FeSe ,² NbSe_2 ,¹¹ NbTe_4 ,¹² and MoTe_2 ¹³ are a few examples of superconducting chalcogenides. In the past few decades, metal chalcogenides with narrow band gaps and low thermal conductivities have been of interest for their promising thermoelectric properties. Examples include AkM_2Te_4 ($\text{Ak} = \text{Sr}, \text{Ba}, M = \text{Sc}, \text{Y}$),¹⁴ $\text{BaCu}_{2-x}\text{Ag}_x\text{Te}_2$,¹⁵ $\text{Ba}_3\text{Cu}_{14-x}\text{Te}_{12}$,¹⁶ and YCuTe_2 .¹

The structural chemistry of metal chalcogenides is also very rich. Many of the metal chalcogenides are layered, but there are more complicated structures ranging from zero-dimensional to three-dimensional. The chalcogen ($Q = \text{S}, \text{Se},$ and Te) atoms in these structures often show homoatomic bonding with a variety of Q_n^{x-} units, something not possible with oxides. The tendency of chalcogens to form $\text{Q}\cdots\text{Q}$ units is relatively more prominent for Te than for S or Se atoms.¹⁷ Thus, a large number of metal tellurides crystallize in the new structure types with intricate structures. The Te atoms in these metal tellurides form a wide range of polyanions (Q_n^{x-}) starting from the simplest Te_2^{2-} units,¹⁷ oligomeric motifs Te_n^{2-} ,¹⁸ one-dimensional infinite chains of $\text{Te}-\text{Te}-\text{Te}$ (e.g., $\text{LaCu}_{0.40}\text{Te}_2$,¹⁹ $\text{GdCu}_{0.33}\text{Te}_2$,¹⁹ and $\text{Gd}_3\text{Cu}_2\text{Te}_7$ ²⁰), and square nets of Te atoms in $\text{Cu}_{0.66}\text{EuTe}_2$,²¹ $\text{KCu}_2\text{EuTe}_4$,²¹ $\text{Na}_{0.2}\text{Ag}_{2.8}\text{EuTe}_4$,²¹ and $\text{K}_{0.33}\text{Ba}_{0.67}\text{AgTe}_2$.²² The compositions of such new tellurides are difficult to predict. Thus, exploratory solid state-synthesis is the most effective route to the discovery of new chalcogenides with interesting structures and properties.

The ternary Ak–Sc–Te system (Ak = Mg, Ca, Sr, and Ba) contains only two compounds, BaSc₂Te₄ and SrSc₂Te₄, that adopt the well-known CaFe₂O₄ structure type.¹⁴ In this report, we present the synthesis and crystal structure of the first polytelluride Ba₃ScTe₅ of the Ak–Sc–Te ternary system. Its structure is modulated. The subcell structure of this compound features linear infinite Te–Te–Te chains. We have also studied the physical properties of Ba₃ScTe₅, including optical bandgap and temperature-dependent resistivity studies along with its electronic structure.

EXPERIMENTAL METHODS

Syntheses. *Caution!* ²³⁸U is an α -emitting radioisotope and as such is considered a health risk. Its use requires appropriate infrastructure and personnel trained in the handling of radioactive materials.

The following reactants were used as obtained: Ba (Johnson Matthey, 99.5 %), Te (Aldrich, 99.8 %), and Sc (Alfa Aesar, 99.9 %). Depleted U powder was obtained by hydridization and decomposition of turnings (IBI Labs) in a modification²³ of a previous literature method.²⁴

“U-assisted” Synthesis of Crystals of Ba₃ScTe₅. The black irregular-shaped crystals of Ba₃ScTe₅ were first obtained from a reaction of Ba (34.6 mg, 0.252 mmol), U (10.0 mg, 0.042 mmol), Sc (3.8 mg, 0.084 mmol), and Te (85.8 mg, 0.672 mmol) during exploration of the quaternary Ba/Sc/U/Te system. The reactants were weighed inside an Ar-filled dry box. The reaction mixture was transferred into a carbon-coated fused-silica tube that was then evacuated and flame sealed under a vacuum (*ca.* 10⁻⁴ Torr). The tube was placed in a programmable furnace for heat treatment. The temperature of the furnace was first ramped up to 1043 K in 24 h, and then the reaction was allowed to equilibrate at this temperature for 24 h before ramping up the temperature to 1173 K in 24 h. The temperature of the furnace was held constant at 1173 K for 199 h, and finally the reaction mixture was allowed to cool down to 373 K in 263 h. The composition of the products of the reaction was analyzed using the energy dispersive X-ray analysis (EDX) with the use of a Hitachi S3400 scanning electron microscope. The EDX study on black irregular shaped crystals showed the presence of Ba₃ScTe₅ (Ba:Sc:Te \approx 3:1:5). The

secondary phases present in the reaction product were black plate-shaped crystals of UOTe (U:Te \approx 1:1),²⁵ and yellow blocks of BaTe (Ba:Te \approx 1:1).²⁶

Rational Synthesis of Crystals of Ba₃ScTe₅. The crystals of Ba₃ScTe₅ were successfully synthesized by loading the stoichiometric amounts of Ba (94.1 mg, 0.69 mmol), Sc (10.3 mg, 0.23 mmol), and Te (145.7 mg, 1.14 mmol) into a carbon-coated fused-silica 6 mm (inner diameter) tube inside an Ar filled glove box. The tube was sealed with a flame torch under vacuum (*ca.* 10⁻⁴ Torr) and then it was placed vertically in an alumina crucible inside the computer-controlled chamber furnace. The following heating profile was used: The temperature was ramped up to 1223 K within 36 h and then the tube was annealed there for 96 h. After that, the reaction mixture was cooled to 772 K at the rate of 3.98 K/h and finally the furnace was turned off. After the completion of the reaction, a black solid lump was obtained. Black irregular-shaped crystals of Ba₃ScTe₅ were found after breaking the black lump. Also present were BaTe crystals.

Synthesis of Polycrystalline Ba₃ScTe₅. The polycrystalline sample of Ba₃ScTe₅ was synthesized for physical property measurement by loading stoichiometric amounts of Ba (188.13 mg, 1.370 mmol), Sc (20.529 mg, 0.456 mmol), and Te (291.34 mg, 2.283 mmol) in a carbon-coated fused-silica tube under an Ar atmosphere inside a glove box. The tube was evacuated (*ca.* 10⁻⁴ Torr) and sealed. Then the tube was kept in a programmable muffle furnace and was heated to 1173 K in 36 hours. It was kept at 1173 K for four days and then the furnace was switched off. Next the cooled product was ground into fine powder inside the Ar-filled glove box. From the PXRD study, the polycrystalline product was found to be almost single phase Ba₃ScTe₅ along with a minute amount of cubic BaTe.

Crystal Structure Determination. The single-crystal X-ray diffraction data on Ba₃ScTe₅ crystal that was obtained by the “U-assisted reaction” were collected at 100(2) K with the use of a Bruker APEX2 kappa diffractometer equipped with graphite-monochromized Mo-K α radiation ($\lambda = 0.71073$ Å). The data collection strategy was optimized with the use of the algorithm COSMO in the APEX2 package as a series of ω and φ scans.²⁷ Scans of 0.3° at 20

s/frame were used. The detector to crystal distance was 50 mm. The collection of intensity data as well as cell refinement and data reduction were carried out with the use of the program APEX2.²⁷ Precession images of the data set showed additional satellite reflections indicative of a modulated structure. The substructure of Ba₃ScTe₅ was solved and refined in a straightforward manner in the hexagonal space group *P6₃/mcm* with the use of the SHELX-14 algorithms of the SHELXTL program package.^{28,29} Face indexed absorption, incident beam, and decay corrections of the substructure were performed with the use of the program SADABS.²⁹ The thermal parameter of one of the crystallographically independent Te atom was found to be cigar-shaped. The program STRUCTURE TIDY³⁰ in PLATON³¹ was used to standardize the atomic positions of the substructure.

Table 1. Crystallographic Data and Structure Refinement Details for the Substructure of Ba₃ScTe₅.

	Ba ₃ ScTe ₅
Temperature (K)	100(2)
<i>a</i> (Å)	10.1190(5)
<i>c</i> (Å)	6.8336(3)
<i>V</i> (Å ³)	605.98(7)
ρ (g cm ⁻³)	6.001
μ (mm ⁻¹)	21.89
<i>R</i> (<i>F</i>) ^b	0.029
<i>R</i> _w (<i>F</i> _o ²) ^c	0.067

^aSpace group is *D*³_{6h}-*P6₃/mcm*, $\lambda = 0.71073$ Å, *Z* = 2.

^b*R*(*F*) = $\Sigma ||F_o| - |F_c|| / \Sigma |F_o|$ for $F_o^2 > 2\sigma(F_o^2)$.

^c*R*_w(*F*_o²) = $\{\Sigma [w(F_o^2 - F_c^2)^2] / \Sigma wF_o^4\}^{1/2}$. For $F_o^2 < 0$, $w^{-1} = \sigma^2(F_o^2)$; for $F_o^2 \geq 0$, $w^{-1} = \sigma^2(F_o^2) + (qF_o^2)^2$ where $q = 0.0059$ for data collected at 100(2) K.

Face-indexed absorption corrections for the incommensurate supercell were performed with the programs X-SHAPE2³² and JANA2006.³³⁻³⁵ Further details are given in Tables 1, 2, and 3 and in the Supporting Information.

Table 2. Crystallographic Data and Structure Refinement Details for the Modulated structure of Ba₃ScTe₅.

	Ba ₃ ScTe ₅
Formula weight	1095
Temperature	100(2) K
Wavelength	0.71073 Å
Crystal system	Hexagonal
Space group	<i>P</i> -6(00γ)0
Unit cell dimensions	<i>a</i> = 10.1188(3) Å <i>b</i> = 10.1188(3) Å <i>c</i> = 6.8332(3) Å
<i>q</i> -vector(1)	0.3718(2) <i>c</i> *
Volume	605.92(4) Å ³
Density (calculated)	6.0017 g/cm ³
Absorption coefficient	21.888 mm ⁻¹
F(000)	898
θ range for data collection	2.32 to 35.8°
Index ranges	-14 ≤ <i>h</i> ≤ 12, -4 ≤ <i>k</i> ≤ 16, -10 ≤ <i>l</i> ≤ 10, -1 ≤ <i>m</i> ≤ 1
Reflections collected	21514 (7176 main + 14338 satellites)
Independent reflections	4804 (1670 main + 3134 satellites) [<i>R</i> _{int} = 0.0613]
Completeness to θ = 33.29°	98 %
Refinement method	Full-matrix least-squares on <i>F</i> ²
Data / constrains / restrains / parameters	4804 / 2 / 0 / 87

Goodness-of-fit on F^2	0.88
Final R indices ^a [$I > 3\sigma(I)$]	$R_{obs} = 0.0292$, $wR_{obs} = 0.0384$
R indices [all data]	$R_{all} = 0.0801$, $wR_{all} = 0.0447$
Final R main indices [$I > 3\sigma(I)$]	$R_{obs} = 0.0251$, $wR_{obs} = 0.0351$
R main indices (all data)	$R_{all} = 0.0426$, $wR_{all} = 0.0374$
Final R 1 st order satellites [$I > 3\sigma(I)$]	$R_{obs} = 0.0392$, $wR_{obs} = 0.0667$
R 1 st order satellites (all data)	$R_{all} = 0.1457$, $wR_{all} = 0.0966$
Extinction coefficient	820(30)
T_{min} and T_{max} coefficients	0.5173 and 0.7419
Largest diff. peak and hole	4.79 and $-5.38 \text{ e}^- \text{ \AA}^{-3}$

$$R = \frac{\sum ||F_o| - |F_c||}{\sum |F_o|}, wR = \left\{ \frac{\sum [w(|F_o|^2 - |F_c|^2)^2]}{\sum [w(|F_o|^4)]} \right\}^{1/2} \text{ and } w = 1/(\sigma^2(I) + 0.000016I^2).$$

Powder X-ray Diffraction Measurement (PXRD). PXRD studies at 298(2) K were used to confirm the phase purity of the polycrystalline samples. Cu-K α radiation ($\lambda = 1.5406 \text{ \AA}$) was used in the diffractometer (Model: X'Pert Pro-PAN analytical) equipped with an Xcelerator detector. The finely ground polycrystalline sample was fixed at a flat sample stage. The X'Pert High Score software was used to collect the PXRD data in the 2θ range of $10\text{--}70^\circ$ with step size and scan time of 0.01° and 50 min, respectively. The *Match3!* software suite (version 3.6.1) was used to analyze the PXRD patterns.

Solid-State Ultra Violet-Visible Near Infrared Spectroscopy. A PerkinElmer UV/VIS/NIR spectrophotometer was used to study the optical band gap of polycrystalline Ba₃ScTe₅ at 298(2) K in the diffuse reflectance mode over the wavelength range of 1500 nm to 200 nm. BaSO₄ was dried overnight to remove undesired moisture and then was used as a standard reference. The absorption data were generated from the reflectance data using the Kubelka-Munk equation.³⁶

$$\alpha/S = (1 - R)^2/2R \quad (1)$$

Here α , R , and S denote the absorption coefficient, reflectance coefficient, and scattering coefficient, respectively. The Tauc plot was used to estimate the band gap:

$$(\alpha h\nu)^n = A(h\nu - E_g) \quad (2)$$

Here the symbols h , ν , n , A , and E_g stand for Planck's constant, frequency of light, a constant that decides the band gap nature, proportionality constant, and band gap, respectively. The $n = 2$ value signifies a direct band gap and $n = 1/2$ signifies an indirect band gap.

Temperature-Dependent Resistivity Studies. The resistivity data as a function of temperature were collected on a polycrystalline compact pellet of Ba_3ScTe_5 . The circular pellet with a thickness of ≈ 1.4 mm and a diameter of 8 mm was obtained by compacting the polycrystalline powder by applying a pressure of ≈ 10.3 MPa. The resulting compacted disk was further sintered at 923 K inside an evacuated carbon-coated fused-silica tube for ten hours. Four-probe resistivity data were measured between 75 K and 300 K using equipment and procedures described previously.³⁷

Electronic Structure Calculations. The calculations were carried out with the VASP (Vienna ab Initio Simulation Package)^{38,39} code that implements DFT (density functional theory)^{40,41} within the projector augmented wave method.⁴² The DFT method has proven to be one of the most accurate methods for the computation of the electronic structure of solids.⁴³⁻⁴⁵ First, the crystal structure was relaxed using the Perdew, Burke, and Ernzerhof (PBE) functional,⁴⁶ and then the density of states were obtained with the Heyd, Scuseria, and Ernzerhof⁴⁷⁻⁴⁹ (HSE) functional. To ensure the convergence of the calculations, a k -points grid of $8 \times 8 \times 6$ was used for both HSE and PBE calculations. For the HSE calculation, the energy cut-off describing the plane-wave expansion in the wave function was set to the default value of 187.2 eV, while for the PBE relaxation of the structure it was set to 1000 eV. The DFT optimized lattice parameters $a = b = 10.27$ Å and $c = 6.96$ Å are in a reasonable agreement with the experimental values of the substructure ($a = b = 10.1190(5)$ Å and $c = 6.8336(3)$ Å).

RESULTS AND DISCUSSION

Syntheses. The black crystals of the ternary compound Ba_3ScTe_5 were first discovered serendipitously during the exploration of the quaternary Ba/U/Sc/Te system in a small yield of 20 wt% (based on Sc). Further, the synthesis of crystals of Ba_3ScTe_5 was reproduced using the stoichiometric reaction of the corresponding elements at 1223 K followed by slow-cooling to 298 K using the sealed-tube method. This reaction produced a better yield of Ba_3ScTe_5 crystals (*ca.* 80 wt.%). A similar reaction that was aimed for the synthesis of a bulk polycrystalline sample of Ba_3ScTe_5 was also carried out at 1173 K.

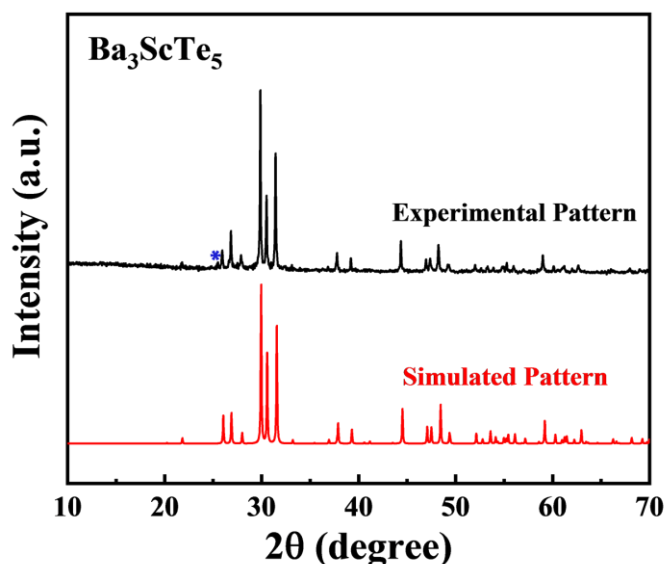


Figure 1: PXRD pattern of the polycrystalline Ba_3ScTe_5 compound. The symbol * indicates reflection from the secondary BaTe phase.

The PXRD pattern of the reaction product showed almost a single phase of Ba_3ScTe_5 along with a very small amount of a secondary cubic BaTe phase (Figure 1). The reheating of the product at 1173 K as a compacted pellet did not improve the phase purity of the polycrystalline sample. We also attempted to make new ternary isostructural phases by replacing Ba with Pb and also replacing Ba with smaller alkaline-earth metals (Ca, Sr), but only binary phases resulted. Also, the replacement of Sc metal with Y metal (Ba_3YTe_5) afforded only binaries of the corresponding elements.

Structure of the Subcell of Ba₃ScTe₅. The subcell structure of Ba₃ScTe₅ (Figure 2) is related to the well-known Hf₅Sn₃Cu⁵⁰ structure type with the Ba atoms at Sn sites, Te atoms at Hf sites, and Sc atoms at Cu sites. Many intermetallic compounds with the Hf₅Sn₃Cu⁵⁰ type structure are known in the literature, but to the best of our knowledge this structure type is not known for any metal chalcogenides. Although, there are few reports on the synthesis of sulfur and selenium doping in binary compounds La₅Ge₃, La₅Pb₃, and Zr₅Sb₃ that adopt the Hf₅Sn₃Cu type structure but their crystal structures and amount of chalcogens doped in these compounds were not established, and only unit cell parameters of these chalcogen doped compounds were reported.⁵¹⁻⁵³ The crystal structure of subcell of Ba₃ScTe₅ comprises of two formula units in the hexagonal space group $D_{3,6h}^3-P6_3/mcm$ with one crystallographic independent Sc site (site symmetry: $-3.m$), one Ba site ($m2m$), and two Te sites [Te1 ($m2m$) and Te2 (3.2)]. Crystal structure refinement details and metric data for the Ba₃ScTe₅ substructure are presented in Table 1 and 3, respectively. Sc atoms in this structure are coordinated to six Te atoms ($6 \times \text{Te1}$) that are arranged in an octahedral fashion around the central metal atom.

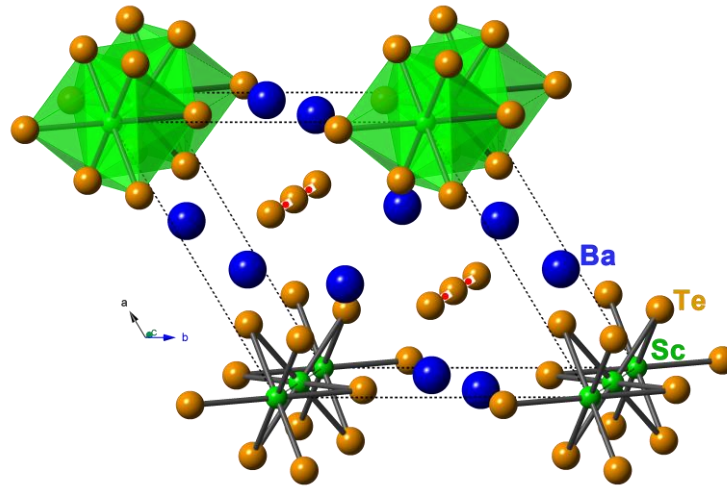


Figure 2: A general view of the structure of subcell of Ba₃ScTe₅ viewed approximately along the c -axis. Here and in succeeding figures Ba, Sc, and Te atoms are shown in blue, green, and orange, respectively.

Each ScTe₆ octahedron is fused to two neighboring ScTe₆ octahedra through sharing of two opposite triangular faces resulting in the formation of an infinite one-dimensional chain of $1, \infty$

[ScTe₃³⁻] along the [001]-direction (Figure 3a). In general, the face-sharing of polyhedral units is considered as least stable as compared with edge- and vertex-sharing of the polyhedra because the two metal atoms are closest in face-sharing. A survey of Sc chalcogenides using the ICSD web program⁵⁴ suggested only one example, RbSc₅Te₈,⁵⁵ where both face- and edge-sharing of Sc-based octahedra can be seen. However, the present ternary phase, Ba₃ScTe₅, is the first example of a Sc telluride where only face-shared ScTe₆ octahedra are present. The six Te1 atoms form an almost perfect octahedral environment around Sc with the Sc–Te1 bond distances of 2.957(1) Å. The Te–Sc–Te angles of these octahedra are also very close to the ideal octahedron with *m*–*3m* symmetry (Table 3). A comparison of Sc–Te distances in Ba₃ScTe₅ with the corresponding distances found in the related structures such as BaSc₂Te₄ (2.878(2)–2.958(1) Å),¹⁴ SrSc₂Te₄ (2.892(1)–2.977(1) Å),¹⁴ RbSc₅Te₈ (2.890(1)–2.926(1) Å),⁵⁵ and TlScTe₂ (2.9341(6) Å)⁵⁶ reveals good agreement with the single Sc³⁺–Te bonding.

Table 3. Selected Interatomic Lengths (Å) in the Substructure of Ba₃ScTe₅.

Atom pair and bond angles	Distance (Å) and angles(deg)
Sc1–Te1	2.9568(7) × 6
Ba1–Te1	3.4047(7) × 2 3.7240(5) × 2 3.8114(13) × 1
Ba1–Te2	3.5790(3) × 4
Te2…Te2	3.417(1)
Te1…Te1	4.180(1)
Sc1…Sc1	3.4168(2) × 2
Ba1…Sc1	4.2526(8) × 4

$$\begin{aligned}
\text{Te}(1) \cdots \text{Sc}(1) \cdots \text{Te}(1) & 90.043(14) \times 6 \\
& 89.957(14) \times 6 \\
& 180.000(19) \times 1 \\
& 180.0 \times 2
\end{aligned}$$

As discussed earlier, the ${}^1_{\infty}[\text{ScTe}_3^{3-}]$ chains are formed by sharing of triangular faces of ScTe_6 octahedra (Figure 3a). As a consequence of face-sharing, the $\text{Sc} \cdots \text{Sc}$ distances are expected to be shorter than those in related structures that have edge-sharing or corner-sharing units of Sc octahedra. Indeed, the $\text{Sc} \cdots \text{Sc}$ interactions of 3.4167(1) Å in Ba_3ScTe_5 are shorter when compared with TlScTe_2 (4.2128(4) Å),⁵⁶ BaSc_2Te_4 (4.2692(1) Å),¹⁴ and $\text{CsCu}_2\text{Sc}_3\text{Te}_6$ (4.0430(1) Å)⁵⁷ that have edge-shared ScTe_6 octahedra. Only RbSc_5Te_8 shows a $\text{Sc} \cdots \text{Sc}$ interaction of 3.6590(1) Å, which is closer to the corresponding interactions in Ba_3ScTe_5 . There are few reports of Sc ternary compounds e.g., Sc_6MTe_2 , [M = Cu (3.04(1) Å) and Ag (3.05(1) Å)],⁵⁸ and Sc_6PdTe_2 (3.08(1) Å)⁵⁹ where a Sc–Sc metal bond is present.

Barium atoms are surrounded by a total of nine Te atoms, five Te1 and four Te2 atoms, in a distorted tricapped trigonal prismatic geometry with Ba–Te distances of 3.405(1) Å to 3.724(1) Å (Figure 3b).

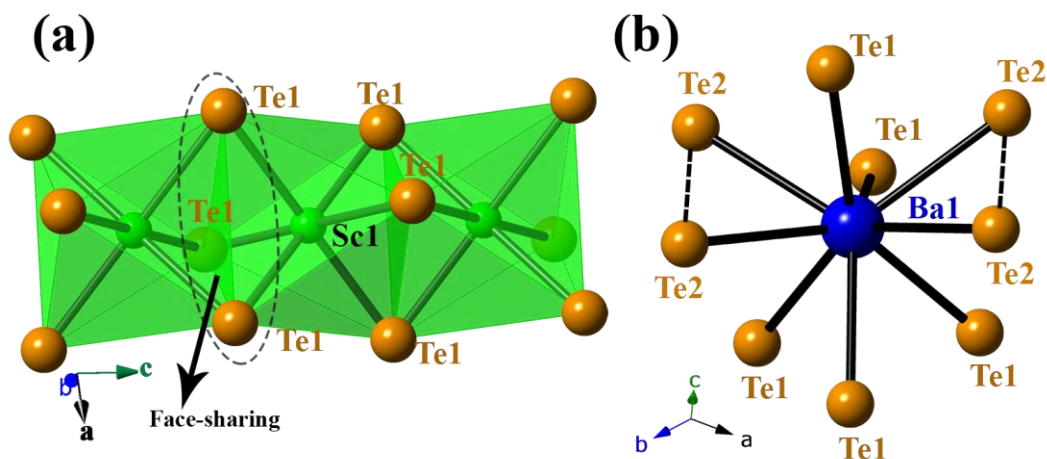


Figure 3: (a) A fragment of the ScTe_6 chain and (b) the local coordination environment of Ba atom in the subcell structure of Ba_3ScTe_5 .

These distances are comparable with the corresponding distances in Ba_2GeTe_5 (3.532(1)–3.711(1) Å),⁶⁰ BaSbTe_3 (3.4064(1)–3.8880(1) Å),⁶¹ and BaBiTe_3 (3.417(2)–3.887(2) Å)⁶² where the local coordination environments of Ba atoms are similar to that of the Ba atoms in Ba_3ScTe_5 . The Te2 atoms form an infinite Te2–Te2–Te2 chain with the shortest Te⋯Te interaction of 3.417(1) Å, longer than the Te–Te single bond length (~2.8 Å) and shorter than the van der Waals interactions of 4.10 Å.

Modulated Structure Description of Ba_3ScTe_5 . The superstructure was refined with JANA2006 software using a hexagonal unit cell with $a = 10.1188(3)$ Å and $c = 6.8332(3)$ Å and a modulation vector of $q = 0.3718(2)c^*$. The only hexagonal space group that gave a satisfactory refinement consistent with the extinction conditions of the observed reflections was $P-6(00\gamma)0$. The asymmetric unit of the modulated superstructure of Ba_3ScTe_5 contains two Ba (site symmetry of both: $m..$), four Te [Te1 and Te2 ($m..$), Te3 and Te4 ($3..$)], and one Sc atom ($3..$). Sc atoms in the structure are bonded to six Te atoms in a distorted octahedral geometry to form infinite chains of $[\text{ScTe}_3^{3-}]$. These $[\text{ScTe}_3^{3-}]$ chains are separated by Ba^{2+} ions and linear chains of Te atoms that are oriented along the c -axis. Infinite chains of Te are distorted because of the formation of long- and short-bonded pairs of Te atoms.

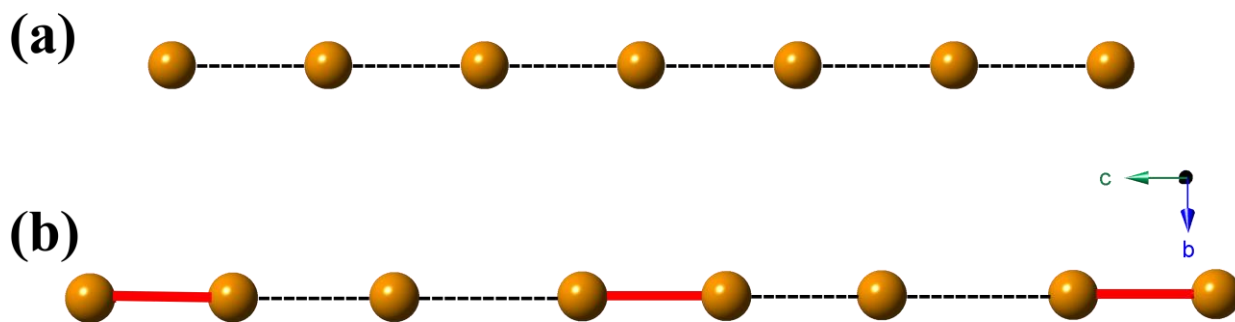


Figure 4: A local view of infinite $-\text{Te}-\text{Te}-\text{Te}-$ chains in (a) the subcell structure and (b) the modulated superstructure of Ba_3ScTe_5 . The Te⋯Te interactions are shown as black dashed lines and Te–Te bonds are shown as solid red lines. The Te–Te bonding threshold is 2.8–2.9 Å.

Presumably, the origin of the observed incommensurate ordering is the result of these Te–Te interactions in the linear chains of Te. The distribution of the Te–Te distances in the linear chains ranges from 2.824(7) Å to 3.955(7) Å, Figure 4. The corresponding Te–Te distances in the

undistorted substructure (when the supercell reflections are omitted from the refinement) is 3.417(1) Å.

Structural Relationship of the Substructure of Ba₃ScTe₅ with Hf₅Sn₃Cu and Mn₅Si₃.

A comparison of Hf₅Sn₃Cu and Mn₅Si₃ structures with the substructure of Ba₃ScTe₅ is shown in Figure 5. The Mn₅Si₃ structure can be considered as a parent structure of both Hf₅Sn₃Cu structure and the Ba₃ScTe₅ substructure. The Mn₅Si₃ structure also crystallizes in the hexagonal space group *P6₃/mcm* with three independent crystallographic sites: Mn1, Mn2, and Si1 with site symmetries of 3.2, *m2m*, and *m2m*, respectively. Mn1 atoms in this structure form the infinite linear chains of Mn1 atoms whereas Mn2 atoms form slightly distorted octahedral shaped clusters of Mn₆ that are face-shared along the *c*-direction. The centers of the Mn2 based octahedra are vacant i.e. Mn₅Si₃ may be rewritten as Mn₅Si₃□₁ where □ represents vacant site with $-3.m$ symmetry (*2b* sites). The Hf₅Sn₃Cu structure (space group: *P6₃/mcm*)⁵⁰ can be considered as a filled variant of Mn₅Si₃□₁ structure.⁶³

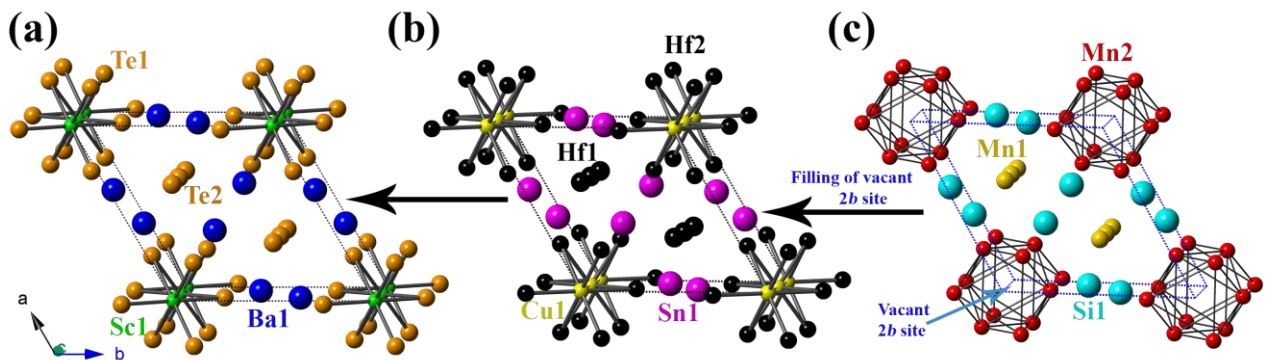


Figure 5: Relations among the subcell structure of (a) Ba₃ScTe₅ with the (b) Hf₅Sn₃Cu⁵⁰ and (c) Mn₅Si₃⁶³ structures.

As can be seen from Figure 5, the Hf atoms are at the Mn positions and Sn atoms are at the Si positions. The Cu atoms fill the vacant □ positions (*2b* sites) i.e. these atoms are situated at the center of octahedra formed by Hf2 atoms. The Ba₃ScTe₅ substructure can be obtained by replacing Cu with Sc1 and Hf2 with Te1, and Hf1 atoms with Te2 atoms in Hf₅Sn₃Cu. The Ba₃ScTe₅ structure is of “anti”-Hf₅Sn₃Cu structure type because of the replacement of electropositive Hf atoms of Hf₅Sn₃Cu structure with electronegative Te atoms in Ba₃ScTe₅.

Oxidation States and Bond Valence Sum (BVS) Calculations. The assignment of formal oxidation states in the Ba_3ScTe_5 substructure is not straightforward because of the presence of $\text{Te}\cdots\text{Te}\cdots\text{Te}$ infinite chains with $\text{Te}\cdots\text{Te}$ interactions that are shorter than the van der Waal's distance and longer than the typical $\text{Te}-\text{Te}$ single bond ($\sim 2.8 \text{ \AA}$). There are numerous examples of metal tellurides where the assignment of oxidation states of Te atoms is complicated and somewhat arbitrary because of such intermediate $\text{Te}\cdots\text{Te}$ interactions e.g., LnTe_3 (Ln = lanthanides),⁶⁴ LnCu_xTe_2 (Ln = La, Nd, Sm, Gd, Dy),¹⁹ $\text{Gd}_3\text{Cu}_2\text{Te}_7$,²⁰ $\text{Ba}_2\text{MAnTe}_7$ (M = Ti, Cr, An = Th, U),⁶⁵ KTh_2Te_6 ,⁶⁶ BaAnTe_4 (An = Th and U),⁶⁷ and ATiU_3Te_9 (A = Rb and Cs).⁶⁸

The assignments of +2 and +3 oxidation states to Ba and Sc atoms, respectively are clear in the Ba_3ScTe_5 substructure. However, the assignment of charges on Te atoms is challenging. As discussed earlier, the Ba_3ScTe_5 substructure contains two types of Te atoms: Te1 atoms that are bonded with Sc atoms and Te2 atoms that are form the infinite $\text{Te}\cdots\text{Te}\cdots\text{Te}$ chains with intermediate $\text{Te}\cdots\text{Te}$ interactions. Hence, the charge on each Te1 atoms could be assigned as $-2 e^-$. This assignment results in an average nonintegral charge of $-1.5 e^-$ on each Te2 atom, i.e., the Te2 atoms are partially reduced in this Ba_3ScTe_5 substructure. The bond valence sum⁶⁹ calculations for Ba_3ScTe_5 substructure using Expo2014 software⁷⁰ yields the following bond valances: 2.36 for Ba1, 2.55 for Sc, 2.17 for Te1, and 1.56 for Te2. The BVS calculation also indicates a partial reduction of Te2 atoms. The modulated structure of Ba_3ScTe_5 shows the splitting of these $\text{Te}\cdots\text{Te}\cdots\text{Te}$ chains into Te_2^{n-} dimers with $\text{Te}-\text{Te}$ minimum and maximum distances of 2.8(1) and 3.9(1) \AA , respectively. The modulated structure contains approximately one dimer per three Te atoms (Figure 4b). There is no evidence of Te vacancies so that the dimerization model can account for the extra electron if all five Te atoms were isolated (Figure 4b). This stabilization of the Ba_3ScTe_5 structure is not possible with Te_2^{2-} dimers instead of distorted $\text{Te}\cdots\text{Te}\cdots\text{Te}$ chains as it demands Ba in +1 state or Sc in +2 state. Hence, we conclude that the presence of these distorted chains of Te with an average charge of $-1.5 e^-$ per Te atom is responsible for stabilization of Ba_3ScTe_5 in the $\text{Hf}_5\text{Sn}_3\text{Cu}$ structure type.

Thus, based on the coordination environments and the distances between the homo/hetero atoms, charge balance in the valence-imprecise Ba_3ScTe_5 structure can be formulated as $(\text{Ba}^{2+})_3(\text{Sc}^{3+})(\text{Te}^{2-})_3(\text{Te}^{1.5-})_2$. An average charge of $-1.5 e^-$ on the Te atoms of the infinite

Te···Te···Te chains in BaAnTe₄ is also known.⁶⁷ Such assignment of non-integer charge of Te atoms of Te···Te···Te chains is common and is reported for many of the tellurides including the Ba₂MAnTe₇ (M = Ti, Cr, An = Th, U)⁶⁵, Cu_xUTe₃,⁷¹ and ATiU₃Te₉ structures.⁶⁸

Optical Band Gap Study. The absorption spectrum (Figure 6) for a polycrystalline sample of Ba₃ScTe₅ was collected at 298(2) K. A broad absorption transition around 0.6(2) eV is apparent from Figure 6a. A direct bandgap of 1.1(2) eV was estimated from the analysis of the square of absorption data as a function of energy (Figure 6b). The value of indirect bandgap was found to be below the instrument limit (~0.8 eV).

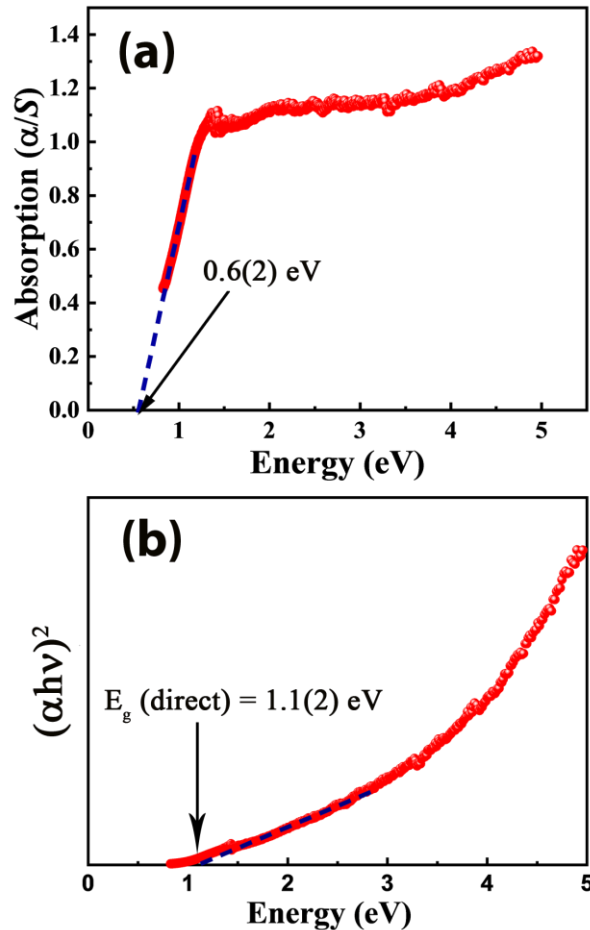


Figure 6: (a) Optical absorption spectrum and (b) solid-state UV/Vis direct bandgap Tauc plot for polycrystalline Ba₃ScTe₅.

This experimental optical band gap, which is consistent with the black color of the compound, suggests that Ba_3ScTe_5 is a semiconductor.

Temperature-Dependent Resistivity Study. The resistivity of polycrystalline Ba_3ScTe_5 as a function of temperature shows an exponential drop in resistivity values with increasing temperature in the range 75 K to 300 K (Figure 7).

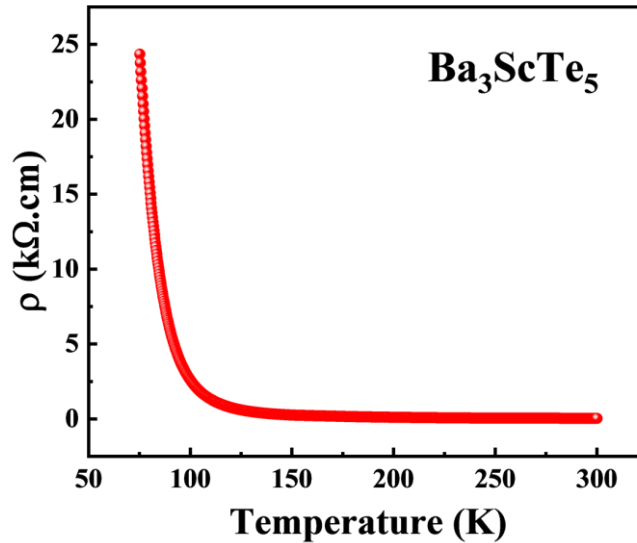


Figure 7: Temperature-dependent resistivity plot for polycrystalline Ba_3ScTe_5 .

The resistivity value of Ba_3ScTe_5 varies between ~ 24 k Ω .cm (at 75 K) and 0.03 k Ω .cm (at 300 K). This behavior is a characteristic of a semiconducting material and is consistent with the optical band gap study of the polycrystalline Ba_3ScTe_5 sample. The semiconducting nature of Ba_3ScTe_5 also suggests that the infinite Te chains in Ba_3ScTe_5 substructure are in fact distorted as suggested by the Peierls distortion theory.⁷²

Electronic Structure of Substructure of Ba_3ScTe_5 . Our computed total (upper plot) and partial (lower plots) density of states (DOS) for Ba_3ScTe_5 are shown in Figure 8. Contrary to what was found in the experiments, we did not find a true bandgap but rather a pseudo-gap, with a low density of states (see total DOS plot) between -1.1 eV and 0.2 eV, with the states present in the pseudo-gap derived mostly from the Te2 atoms (see the corresponding partial DOS).

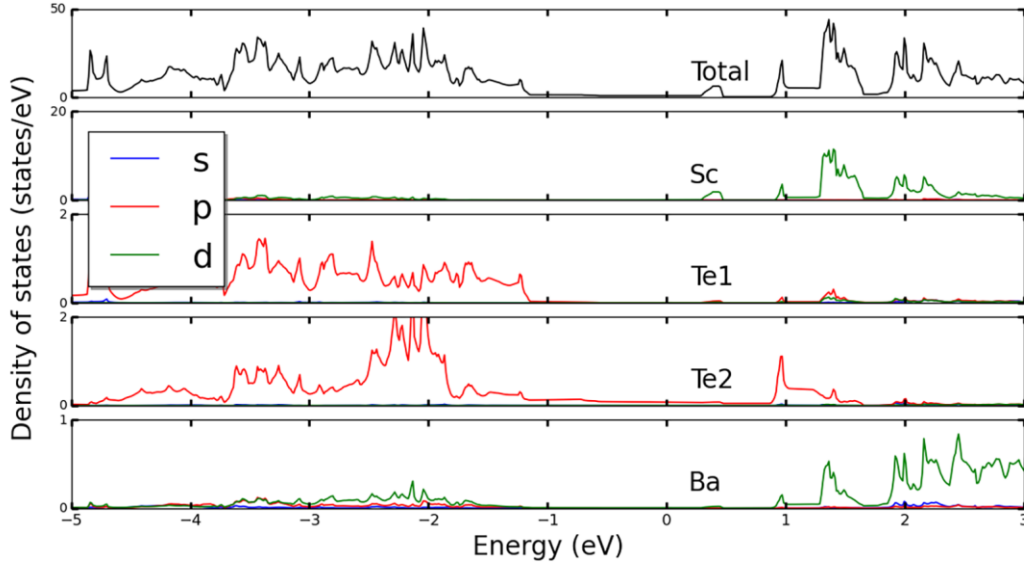


Figure 8: Computed total (upper plot) and partial (lower plots) density of states (DOS) for the subcell structure of Ba_3ScTe_5 . The DOS calculations were performed using the HSE functional.

This difference between a true electronic band gap and a pseudo-gap might arise because the substructure of Ba_3ScTe_5 used for the calculations has linear infinite Te chains that are distorted in the modulated superstructure and could give a weak metallic character to the system.

CONCLUSIONS

Black single crystals of the new ternary polytelluride, Ba_3ScTe_5 , were synthesized at 1173 K. The crystal structure of Ba_3ScTe_5 was determined by a single-crystal X-ray diffraction study at 100(2) K. The precession images simulated from the diffraction data indicate a complex modulated structure for Ba_3ScTe_5 . The subcell of the structure was solved in the space group $P6_3/mcm$ of the hexagonal crystal system with two formula units per unit cell. The asymmetric unit of the subcell contains four crystallographically independent sites: Ba1, Sc1, Te1, and Te2 with site symmetries of $m2m$, $-3.m$, $m2m$, and 3.2 , respectively. The Sc atoms are octahedrally coordinated to six Te1 atoms. Each ScTe_6 octahedron is connected to two neighboring ScTe_6 units by sharing of faces and this results in the formation of chains of $^{1,\infty}[\text{ScTe}_3^{3-}]$ that are separated by

Ba²⁺ cations. The Te₂ atoms in the substructure of Ba₃ScTe₅ form infinite linear chains with equidistant intermediate Te··Te interactions (3.417(1) Å). The modulated superstructure of Ba₃ScTe₅ was solved in the hexagonal superspace group $P-6(00\gamma)0$ with lattice parameters $a = b = 10.1188(3)$ Å, $c = 6.8332(3)$ Å, and an incommensurate modulation vector of $q = 0.3718(2)c^*$. The superstructure Ba₃ScTe₅ also contains chains of $^{1,\infty}[\text{ScTe}_3^{3-}]$ with the Sc atoms octahedrally bonded to six Te atoms. The infinite Te chains in the modulated superstructure are distorted with long and short bonded pairs of Te atoms. The optical absorption band gap study established the semiconducting nature of polycrystalline Ba₃ScTe₅ with a direct band gap of 1.1(2) eV. The resistivity study of a sintered pellet of Ba₃ScTe₅ as a function of temperature shows semiconducting behavior consistent with the optical absorption study and with the pseudo band gap given by DFT electronic structure calculations.

ASSOCIATED CONTENT

Supporting Information.

CCDC #1951174 and 1950724 contain supplementary crystallographic data for the substructure and superstructure of Ba₃ScTe₅, respectively. These data may be obtained free of charge by emailing data_request@ccdc.cam.ac.uk or by contacting the Crystallographic Data Centre, 12 Union Road, Cambridge CB2 1EZ, UK; fax +44 1223 336033. Included with this submission are the cif and checkcif for the substructure. For the superstructure CCDC is unable to handle modulated structures but the raw fcf data are included with this submission.

AUTHOR INFORMATION

Corresponding Author

*E-mail: ibers@chem.northwestern.edu

ORCID

James A. Ibers: 0000-0002-5418-3645

The authors declare no competing financial interest.

ACKNOWLEDGMENTS

J.P. thanks the Science and Engineering Research Board (SERB), Department of Science and Technology (DST), Government of India, for financial support under an Early Career Research award (Grant ECR/2017/000822) and IIT Hyderabad for seed grant and research facilities. M.I. thanks DST India for research fellowship. G. P. and S. J. thank Ministry of Human Resource Development, IIT Hyderabad for research fellowships. Use was made of the Integrated Molecular Structure Education and Research Center X-ray Facility at Northwestern University, which has received support from the Soft and Hybrid Nanotechnology Experimental Resource (NSF Grant ECCS-1542205), the State of Illinois, and the International Institute for Nanotechnology. The authors also thank Dr. Surya Jammalamadaka and Dwipak P. Sahu from the Department of Physics, IIT Hyderabad, for their help in collecting temperature-dependent resistivity data and UV-vis-NIR study.

REFERENCES

- (1) Aydemir, U.; Pöhls, J.-H.; Zhu, H.; Hautier, G.; Bajaj, S.; Gibbs, Z. M.; Chen, W.; Li, G.; Ohno, S.; Broberg, D.; Kang, S. D.; Asta, M.; Ceder, G.; White, A. M.; Persson, K.; Jain, A.; Snyder, G. J. YCuTe₂: a member of a new class of the thermoelectric materials with CuTe₄-based layered structure. *J. Mater. Chem. A* **2016**, *4*, 2461-2472.
- (2) Margadonna, S.; Takabayashi, Y.; McDonald, M. T.; Kasperkiewicz, K.; Mizuguchi, Y.; Takano, Y.; Fitch, A. N.; Suard, E.; Prassides, K. Crystal structure of the new FeSe_{1-x} superconductor. *Chem. Commun.* **2008**, 5607-5609.

- (3) Park, Y.; Degroot, D. C.; Schindler, J.; Kannewurf, C. R.; Kanatzidis, M. G. $K_2Cu_5Te_5$, a Novel Mixed-Valence Layered Compound with Metallic Properties. *Angew. Chem., Int. Ed. Engl.* **1991**, *30*, 1325-1328.
- (4) Lee, M.; Rosenbaum, T. F.; Saboungi, M. L.; Schnyders, H. S. Band-Gap Tuning and Linear Magnetoresistance in the Silver Chalcogenides. *Phys. Rev. Lett.* **2002**, *88*, 066602.
- (5) Joshi, J.; Hill, H. M.; Chowdhury, S.; Malliakas, C. D.; Tavazza, F.; Chatterjee, U.; Walker, A. R. H. W.; Vora, P. M. Short-range charge density wave order in $2H-TaS_2$. *Phys. Rev. B* **2019**, *99*, 245144.
- (6) Greaney, M. A.; Ramanujachary, K. V.; Teweldemedhin, Z.; Greenblatt, M. Studies on the Linear Chain Antiferromagnets: Ba_2MnX_3 ($X = S, Se, Te$) and Their Solid Solutions. *J. Solid State Chem.* **1993**, *107*, 554-562.
- (7) Sturza, M.; Allred, J. M.; Malliakas, C. D.; Bugaris, D. E.; Han, F.; Chung, D. Y.; Kanatzidis, M. G. Tuning the Magnetic Properties of New Layered Iron Chalcogenides $(BaF)_2Fe_{2-x}Q_3$ ($Q = S, Se$) by Changing the Defect Concentration on the Iron Sublattice. *Chem. Mater.* **2015**, *27*, 3280-3290.
- (8) Bronger, W.; Kyas, A.; Müller, P. The Antiferromagnetic Structures of $KFeS_2$, $RbFeS_2$, $KFeSe_2$, and $RbFeSe_2$ and the Correlation between Magnetic Moments and Crystal Field Calculations. *J. Solid State Chem.* **1987**, *70*, 262-270.
- (9) Chia, X.; Ambrosi, A.; Lazar, P.; Sofer, Z.; Pumera, M. Electrocatalysis of layered Group 5 metallic transition metal dichalcogenides (MX_2 , $M = V, Nb, \text{ and } Ta$; $X = S, Se, \text{ and } Te$). *J. Mater. Chem. A* **2016**, *4*, 14241-14253.
- (10) Kliche, G. Far-Infrared and X-Ray Investigations of the Mixed Platinum Dichalcogenides $PtS_{2-x}Se_x$, $PtSe_{2-x}Te_x$, and $PtS_{2-x}Te_x$. *J. Solid State Chem.* **1985**, *56*, 26-31.
- (11) Pervin, R.; Krishnan, M.; Sonachalam, A.; Shirage, P. M. Coexistence of superconductivity and ferromagnetism in defect-induced $NbSe_2$ single crystals. *J. Mater. Sci.* **2019**, *54*, 11903-11912.

- (12) Yang, X.; Zhou, Y.; Wang, M.; Bai, H.; Chen, X.; An, C.; Zhou, Y.; Chen, Q.; Li, Y.; Wang, Z.; Chen, J.; Cao, C.; Li, Y.; Zhou, Y.; Yang, Z.; Xu, Z.-A. Pressure induced superconductivity bordering a charge-density-wave state in NbTe₄ with strong spin-orbit coupling. *Scientific reports* **2018**, *8*, 6298.
- (13) Qi, Y.; Naumov, P. G.; Ali, M. N.; Rajamathi, C. R.; Schnelle, W.; Barkalov, O.; Hanfland, M.; Wu, S.-C.; Shekhar, C.; Sun, Y.; Süß, V.; Schmidt, M.; Schwarz, U.; Pippel, E.; Werner, P.; Hillebrand, R.; Förster, T.; Kampert, E.; Parkin, S.; Cava, R. J.; Felser, C.; Yan, B.; Medvedev, S. A. Superconductivity in Weyl semimetal candidate MoTe₂. *Nat. Commun.* **2016**, *7*, 11038.
- (14) Assoud, A.; Soheilnia, N.; Kleinke, H. Thermoelectric properties of the new tellurides SrSc₂Te₄ and BaSc₂Te₄ in comparison to BaY₂Te₄. *Intermetallics* **2007**, *15*, 371-376.
- (15) Yang, C.; Guo, K.; Yang, X.; Xing, J.; Wang, K.; Luo, J.; Zhao, J.-T. Realizing High Thermoelectric Performance in BaCu_{2-x}Ag_xTe₂ through Enhanced Carrier Effective Mass and Point-Defect Scattering. *ACS Appl. Energy Mater.* **2019**, *2*, 889-895.
- (16) Assoud, A.; Thomas, S.; Sutherland, B.; Zhang, H.; Tritt, T. M.; Kleinke, H. Thermoelectric Properties of the New Polytelluride Ba₃Cu_{14-δ}Te₁₂. *Chem. Mater.* **2006**, *18*, 3866-3872.
- (17) Ibers, J. Tellurium in a twist. *Nat. Chem.* **2009**, *1*, 508.
- (18) Graf, C.; Assoud, A.; Mayasree, O.; Kleinke, H. Solid State Polyselenides and Polytellurides: A Large Variety of Se-Se and Te-Te Interactions. *Molecules* **2009**, *14*, 3115-3131.
- (19) Huang, F. Q.; Brazis, P.; Kannewurf, C. R.; Ibers, J. A. Syntheses, Structures, Physical Properties, and Theoretical Study of LaCu_{0.40}Te₂, NdCu_{0.37}Te₂, SmCu_{0.34}Te₂, GdCu_{0.33}Te₂, and DyCu_{0.32}Te₂. *J. Am. Chem. Soc.* **2000**, *122*, 80-86.
- (20) Huang, F. Q.; Ibers, J. A. Gd₃Cu₂Te₇ and U₂Cu_{0.78}Te₆: Two Examples of Linear Te Chains. *J. Solid State Chem.* **2001**, *159*, 186-190.

- (21) Patschke, R.; Brazis, P.; Kannewurf, C. R.; Kanatzidis, M. G. $\text{Cu}_{0.66}\text{EuTe}_2$, $\text{KCu}_2\text{EuTe}_4$ and $\text{Na}_{0.2}\text{Ag}_{2.8}\text{EuTe}_4$: compounds with modulated square Te nets. *J. Mater. Chem.* **1999**, *9*, 2293-2296.
- (22) Zhang, X.; Li, J.; Foran, B.; Lee, S.; Guo, H.-Y.; Hogan, T.; Kannewurf, C. R.; Kanatzidis, M. G. Distorted Square Nets of Tellurium in the Novel Quaternary Polytelluride $\text{K}_{0.33}\text{Ba}_{0.67}\text{AgTe}_2$. *J. Am. Chem. Soc.* **1995**, *117*, 10513-10520.
- (23) Bugaris, D. E.; Ibers, J. A. Syntheses, structures, and magnetic and optical properties of the compounds $[\text{Hg}_3\text{Te}_2][\text{UCl}_6]$ and $[\text{Hg}_4\text{As}_2][\text{UCl}_6]$. *J. Solid State Chem.* **2008**, *181*, 3189-3193.
- (24) Haneveld, A. J. K.; Jellinek, F. Some Ternary Uranium Chalcogenides. *J. Less-Common Met.* **1969**, *18*, 123-129.
- (25) Murasik, A.; Suski, W.; Leciejewicz, J. Neutron Diffraction Measurements on Antiferromagnetic UOTe at 4.2 °K. *Phys. Status Solidi* **1969**, *34*, K157-K158.
- (26) R.W.G., W. *Crystal Structures*, Second ed.; Interscience Publishers: New York, 1963; Vol. 1.
- (27) *Bruker APEX2 Version 2009.5-1 Data Collection and Processing Software*; Bruker Analytical X-Ray Instruments, Inc.: Madison, WI, USA, 2009.
- (28) Sheldrick, G. M. A short history of SHELX. *Acta Crystallogr. Sect. A: Found. Crystallogr.* **2008**, *64*, 112-122.
- (29) Sheldrick, G. M. SADABS; Department of Structural Chemistry, University of Göttingen, Göttingen, Germany, 2008.
- (30) Gelato, L. M.; Parthé, E. STRUCTURE TIDY - a computer program to standardize crystal structure data. *J. Appl. Crystallogr.* **1987**, *20*, 139-143.
- (31) Spek, A. L. PLATON, A Multipurpose Crystallographic Tool; Utrecht University, Utrecht, The Netherlands, 2014.

- (32) X-SHAPE, Stoe & Cie, Darmstadt, Germany, 2002.
- (33) Oszlányi, G.; Sütő, A. *Ab initio* structure solution by charge flipping. *Acta Cryst.* **2004**, *A60*, 134-141.
- (34) Oszlányi, G.; Sütő, A. *Ab initio* structure solution by charge flipping. II. Use of weak reflections. *Acta Cryst.* **2005**, *A61*, 147-152.
- (35) Petricek, V.; Dusek, M.; Palatinus, L. Crystallographic Computing System JANA2006: General features. *Z. Kristallogr.* **2014**, *229*, 345-352.
- (36) Kortüm, G. *Reflectance Spectroscopy: Principles, Methods, Applications*; Springer-Verlag: New York, 1969.
- (37) Jana, S.; Ishtiyak, M.; Mesbah, A.; Lebègue, S.; Prakash, J.; Malliakas, C. D.; Ibers, J. A. Synthesis and Characterization of Ba₂Ag₂Se₂Se₂. *Inorg. Chem.* **2019**, *58*, 7837-7844.
- (38) Kresse, G.; Furthmüller, J. Efficiency of ab-initio total energy calculations for metals and semiconductors using a plane-wave basis set. *Comput. Mater. Sci.* **1996**, *6*, 15-50.
- (39) Kresse, G.; Joubert, D. From ultrasoft pseudopotentials to the projector augmented-wave method. *Phys. Rev. B* **1999**, *59*, 1758-1775.
- (40) Kohn, W.; Sham, L. J. Self-Consistent Equations Including Exchange and Correlation Effects. *Phys. Rev.* **1965**, *140*, 1133-1138.
- (41) Hohenberg, P.; Kohn, W. Inhomogeneous Electron Gas. *Phys. Rev.* **1964**, *136*, 864-871.
- (42) Blöchl, P. E. Projector augmented-wave method. *Phys. Rev. B* **1994**, *50*, 17953-17979.
- (43) Reshak, A. H.; Abbass, N. M.; Bila, J.; Johan, M. R.; Kityk, I. Noncentrosymmetric Sulfide Oxide MZnSO (M = Ca or Sr) with Strongly Polar Structure as Novel Nonlinear Crystals. *J. Phys. Chem. C* **2019**, *123*, 27172–27180.
- (44) Huang, H.; Reshak, A. H.; Auluck, S.; Jin, S.; Tian, N.; Guo, Y.; Zhang, Y. Visible-Light-Responsive Sillén-Structured Mixed-Cationic CdBiO₂Br Nanosheets: Layer Structure

- Design Promoting Charge Separation and Oxygen Activation Reactions. *J. Phys. Chem. C* **2018**, *122*, 2661–2672.
- (45) Chen, Y.; Molokeev, M. S.; Atuchin, V. V.; Reshak, A. H.; Auluck, S.; Alahmed, Z. A.; Xia, Z. Synthesis, Crystal Structure, and Optical Gap of Two-Dimensional Halide Solid Solutions $\text{CsPb}_2(\text{Cl}_{1-x}\text{Br}_x)_5$. *Inorg. Chem.* **2018**, *57*, 9531–9537.
- (46) Perdew, J. P.; Burke, K.; Ernzerhof, M. Generalized Gradient Approximation Made Simple. *Phys. Rev. Lett.* **1996**, *77*, 3865–3868.
- (47) Heyd, J.; Scuseria, G. E.; Ernzerhof, M. Hybrid functionals based on a screened Coulomb potential. *J. Chem. Phys.* **2003**, *118*, 8207–8215.
- (48) Heyd, J.; Scuseria, G. E.; Ernzerhof, M. Erratum: "Hybrid functionals based on a screened Coulomb potential" [*J. Chem. Phys.* 118, 8207 (2003)]. *J. Chem. Phys.* **2006**, *124*, 219906.
- (49) Paier, J.; Marsman, M.; Hummer, K.; Kresse, G.; Gerber, I. C.; Angyan, J. G. Screened hybrid density functionals applied to solids. *J. Chem. Phys.* **2006**, *124*, 154709.
- (50) Rieger, W.; Nowotny, H.; Benesovsky, F. Phasen mit oktaedrischen Bauelementen des Übergangsmetalls. *Monatsh. Chem.* **1965**, *96*, 232–241.
- (51) Garcia, E.; Corbett, J. D. Chemistry in the Polar Intermetallic Host, Zr_5Sb_3 . Fifteen Interstitial Compounds. *Inorg. Chem.* **1990**, *29*, 3274–3282.
- (52) Guloy, A. M.; Corbett, J. D. The Lanthanum-Germanium System. Nineteen Isostructural Interstitial Compounds of the La_5Ge_3 Host. *Inorg. Chem.* **1993**, *32*, 3532–3540.
- (53) Guloy, A. M.; Corbett, J. D. Exploration of the Interstitial Derivatives of La_5Pb_3 (Mn_3Si_3 -Type). *J. Solid State Chem.* **1994**, *109*, 352–358.
- (54) Belsky, A.; Hellenbrandt, M.; Karen, V. L.; Luksch, P. New developments in the Inorganic Crystal Structure Database (ICSD): accessibility in the support of materials research and design. *Acta Cryst.* **2002**, *B58*, 364–369.

- (55) Babo, J.-M.; Schleid, T. Synthesis and Crystal Structure of the Rubidium Scandium Telluride RbSc_5Te_8 . *Z. Anorg. Allg. Chem.* **2008**, *634*, 1463-1465.
- (56) Teske, C. L.; Bensch, W.; Mankovsky, S.; Ebert, H. Preparation, Crystal Structure, Physical Properties and Electronic Band Structure of TlScQ_2 (Q = S, Se and Te). *Z. Anorg. Allg. Chem.* **2008**, *634*, 445-451.
- (57) Babo, J.-M.; Schleid, T. $\text{CsCu}_2\text{Sc}_3\text{Te}_6$ and $\text{CsCuY}_2\text{Te}_4$: Two new quaternary cesium copper rare-earth metal tellurides. *Solid State Sci.* **2010**, *12*, 238-245.
- (58) Chen, L.; Corbett, J. D. Synthesis, Structure, and Bonding of Sc_6MTe_2 (M = Ag, Cu, Cd): Heterometal-Induced Polymerization of Metal chains in Sc_2Te . *Inorg. Chem.* **2002**, *41*, 2146-2150.
- (59) Maggard, P. A.; Corbett, J. D. Insights into Metal Framework Constructions from the Syntheses of New Scandium- and Yttrium-Rich Telluride Compounds: $\text{Y}_5\text{Ni}_2\text{Te}_2$ and Sc_6PdTe_2 . *J. Am. Chem. Soc.* **2000**, *122*, 10740-10741.
- (60) Prakash, J.; Mesbah, A.; Lebègue, S.; Ibers, J. A. Synthesis, crystal structure, and electronic structure of $\text{Ba}_2\text{GeTe}_3(\text{Te}_2)$. *Solid State Sci.* **2019**, *97*, 105974.
- (61) Volk, K.; Cordier, G.; Cook, R.; Schäfer, H. BaSbTe_3 und BaBiSe_3 Verbindungen mit BiSe- bzw. SbTe-Schichtverbänden. *Z. Naturforsch. B: Chem. Sci.* **1980**, *35b*, 136-140.
- (62) Chung, D.-Y.; Jovic, S.; Hogan, T.; Kannewurf, C. R.; Brec, R.; Rouxel, J.; Kanatzidis, M. G. Oligomerization Versus Polymerization of Te_x^{n-} in the Polytelluride Compound BaBiTe_3 . Structural Characterization, Electronic Structure, and Thermoelectric Properties. *J. Am. Chem. Soc.* **1997**, *119*, 2505-2515.
- (63) Yusupov, R. G.; Stanley, C. J.; Welch, M. D.; Spratt, J.; Cressey, G.; Rumsey, M. S.; Seltmann, R.; Igamberdiev, E. Mavlyanovite, Mn_5Si_3 : a new mineral species from a lamproite diatreme, Chatkal Ridge, Uzbekistan. *Mineral Mag.* **2009**, *73(1)*, 43-50.

- (64) Muravieva, V. K.; Pomelova, T. A.; Tarasenko, M. S.; Kuratieva, N. V.; Naumov, N. G. Crystal structure of LnTe_3 , where $\text{Ln} = \text{La, Ho}$. *J. Struct. Chem. (Engl. Trans.)* **2017**, *58*, 1676-1680.
- (65) Prakash, J.; Mesbah, A.; Beard, J.; Lebègue, S.; Malliakas, C. D.; Ibers, J. A. Three New Quaternary Actinide Chalcogenides $\text{Ba}_2\text{TiUTe}_7$, $\text{Ba}_2\text{CrUTe}_7$, and $\text{Ba}_2\text{CrThTe}_7$: Syntheses, Crystal Structures, Transport Properties, and Theoretical Studies. *Inorg. Chem.* **2015**, *54*, 3688-3694.
- (66) Wu, E. J.; Pell, M. A.; Ibers, J. A. Synthesis and characterization of KTh_2Se_6 , KTh_2Te_6 and CsTh_2Se_6 . *J. Alloys Compd.* **1997**, *255*, 106-109.
- (67) Prakash, J.; Lebègue, S.; Malliakas, C. D.; Ibers, J. A. Syntheses, Crystal Structures, Resistivity Studies, and Electronic Properties of Three New Barium Actinide Tellurides: BaThTe_4 , BaUTe_4 , and BaUTe_6 . *Inorg. Chem.* **2014**, *53*, 12610-12616.
- (68) Ward, M. D.; Mesbah, A.; Lee, M.; Malliakas, C. D.; Choi, E. S.; Ibers, J. A. Synthesis and Characterization of Two Quaternary Uranium Tellurides, $\text{RbTiU}_3\text{Te}_9$ and $\text{CsTiU}_3\text{Te}_9$. *Inorg. Chem.* **2014**, *53*, 7909-7915.
- (69) Brown, I. D. *The Chemical Bond in Inorganic Chemistry, The Bond Valence Model*; Oxford University Press: New York, 2002.
- (70) Altomare, A.; Cuocci, C.; Giacovazzo, C.; Moliterni, A.; Rizzi, R.; Corriero, N.; Falcicchio, A. EXPO2013: a kit of tools for phasing crystal structures from powder data. *J. Appl. Crystallogr.* **2013**, *46*, 1231-1235.
- (71) Patschke, R.; Breshears, J. D.; Brazis, P.; Kannewurf, C. R.; Billinge, S. J. L.; Kanatzidis, M. G. Cu_xUTe_3 : Stabilization of UTe_3 in the ZrSe_3 Structure Type via Copper Insertion. The Artifact of Te-Te Chains and Evidence for Distortions Due to Long Range Modulations. *J. Am. Chem. Soc.* **2001**, *123*, 4755-4762.
- (72) Peierls, R. *More Surprises in Theoretical Physics*; Princeton University Press: New Jersey, 1991.

For Table of Contents Only

Ba_3ScTe_5 was synthesized and its modulated crystal structure was solved in the hexagonal superspace group $P-6(00\gamma)0$ with $a = 10.1188(3) \text{ \AA}$ and $c = 6.8332(3) \text{ \AA}$, and a modulation vector of $q = 0.3718(2)c^*$. Its structure is made up of infinite chains of $^1_{\infty}[\text{ScTe}_3^{3-}]$ that are separated by Ba^{2+} cations and infinite linear chains of Te atoms that are distorted owing to the formation of long- and short-bonded pairs of Te atoms.

